

Morphology–Interface–Property Relationships in Polystyrene/Ethylene–Propylene Rubber Blends. 2. Influence of Areal Density and Interfacial Saturation of Diblock and Triblock Copolymer Interfacial Modifiers

Stefania Polizu and Basil D. Favis*

CRASP, Department of Chemical Engineering, Ecole Polytechnique de Montreal,
P.O. Box 6079 Station Centre Ville, Montreal, Quebec, Canada H3C 3A7

Toan Vu-Khanh

Département de Génie Mécanique, Faculté des Sciences appliquées, Université de Sherbrooke,
2500, boul. de l'Université, Sherbrooke, Québec, Canada J1K 2R7

Received September 18, 1998; Revised Manuscript Received February 12, 1999

ABSTRACT: An emulsification curve which tracks the change in dispersed phase size with interfacial modifier concentration and a fracture mechanics approach have been used to study the behavior of a variety of well-defined interfacial modifiers for a melt-processed ethylene–propylene rubber (EPR)/polystyrene (PS) blend. In this study two poly(styrene/ethylene–butylene) (SEB) diblock copolymers and a poly(styrene/ethylene–propylene) (SEP) diblock copolymer were compared. All of the above interfacial modifiers demonstrate an excellent emulsification efficacy for the EPR/PS system, and no effect was observed when changing the block structure from ethylene–butylene to ethylene–propylene. Despite the excellent capacity of all three diblock modifiers to emulsify the blend, the Charpy and notched and unnotched Izod impact testing demonstrate significantly different behaviors for the various copolymers. The higher molecular weight SEB ($M_n = 187\,000$) and SEP ($M_n = 140\,000$) interfacial modifiers displayed a brittle fracture behavior over a wide range of interfacial modifier concentrations. The lower molecular weight SEB diblock ($M_n = 67\,000$) displays a brittle to ductile transition in impact closely related to the concentration of modifier required for saturation of the interface. Its ability to improve the properties is due to a high areal density of polymer chains at the interface compared to the two higher molecular weight diblock copolymers as directly estimated from the emulsification curve. These results underline the difficulty of achieving high areal densities of copolymer at the interface in melt-processed systems. In addition, the mechanical performance of this effective lower molecular diblock was compared with a triblock, poly(styrene/ethylene–butylene/styrene) (SEBS), of similar molecular weight. The diblock and triblock copolymers both demonstrate the ability to substantially improve the mechanical properties of PS/EPR once interfacial saturation is achieved and possess a virtually identical behavior despite the fact that the styrene block in the triblock copolymer is below its entanglement molecular weight. The similar performance of the triblock and diblock copolymers appears to be due in large part to a similar areal density of joints across the interface.

Introduction

The vast majority of polymer blends are immiscible and hence display a discrete dispersed phase in a matrix material. Today, there is general agreement that controlling both the interface and the microstructure are the keys to developing novel blend materials.¹ To develop useful materials, an interfacial modifier is either added or generated in situ during melt processing. The modifier must therefore find its way to the interface during melt mixing and situate itself appropriately in order to emulsify the system. It must also interdiffuse sufficiently into the respective homopolymer phases to improve adhesion.

Recently, a series of studies have aimed at understanding adhesion phenomena in immiscible blend systems. Brown et al.^{2,3} and Kramer et al.^{4,5} have studied immiscible polymer blends and developed an approach to evaluate the molecular mechanisms affecting adhesion in these types of systems. They deposited a well-defined copolymer interfacial modifier directly at the interface using a spin-coating technique and then built a laminate sample of both homopolymers and the

interphase. A cantilever beam technique was used to propagate a well-defined crack at the interface. By controlling the level of deuteration of their copolymer, the analysis of the fractured surfaces by spectroscopic techniques was able to determine whether fracture provoked chain scission or chain pullout. In their series of studies they evaluate the critical strain energy release rate, G_c , as a function of a variety of parameters including the influence of the areal density (no. of chains per nm²) of copolymer at the interface. They underline the importance of the copolymer blocks being above their entanglement molecular weight as well as an optimal value of the areal density of copolymer at the interface.

In attempting to extend these results to the case of melt-blended systems, a series of additional questions must be posed. Does the copolymer migrate and effectively situate itself at the interface—in other words, is it a good emulsifier, or is a portion lost in the dispersed phase and the matrix? What are the molecular parameters that most influence emulsification? As well, how can one develop a technique to effectively estimate the areal density of copolymer at the interface

for the case of dispersed particles? In fact, for a melt-blended system it is vital to separate out the role of emulsification from fracture performance.

In classical oil-water emulsions stabilized by surfactants, the efficacy of the interfacial modifier for the interface is often characterized by the so-called emulsification curves, which essentially follow the evolution of dispersed phase size with modifier concentration.⁶ The shape of the emulsification curve is highly dependent on surfactant type and on processing technique.⁷ It has been shown recently that the emulsification curve can be applied widely to polymer blends.⁸⁻¹¹ It displays some key characteristics—an initial significant drop in the size of the dispersed phase with the addition of the copolymer followed by the obtention of an equilibrium diameter value at high concentrations of modifier once interfacial saturation has been obtained. This drop in particle size is the result of reduced coalescence and interfacial tension due to the presence of the interfacial modifier.¹² The emulsification curve can allow one to estimate the quantity of copolymer necessary to achieve interfacial saturation. Assuming that all the modifier is at the interface, the area occupied per modifier molecule or its reciprocal, the areal density of copolymer at the interface (no. of chains per nm²) can then be calculated.

Previous investigations,¹³⁻¹⁵ mostly based on a thermodynamics approach, have provided a good theoretical basis of the factors influencing the efficacy of a given interfacial modifier. However, rigorous experimental treatment of these issues in melt blending operations has only just begun to be treated in the literature. This is the seventh paper in a series^{8,16-20} that has been using PS/EPR as a model system to evaluate emulsification and fracture performance in melt-blended systems. Using emulsification curves, the first papers used a series of well-defined diblock and triblock copolymer interfacial modifiers to examine issues such as the influence of molecular weight, chemical composition, and architecture on emulsification efficacy. For the 90% PS/10% EPR system, the triblock copolymers were found to be excellent interfacial agents.⁸ The chemical composition of the copolymer plays an important role in the system morphology, and the presence of double bonds in the molecule significantly diminishes its emulsification capability. On the other hand, the molecular weight of triblock copolymers did not demonstrate any significant differences in emulsification efficacy. Three copolymers of widely different molecular weight displayed similar critical concentrations for interfacial saturation and similar equilibrium particle sizes.

The 80% PS/20% EPR system was used to compare the efficiency of diblock and triblock copolymers.^{16,18} For the diblock copolymers a small molecular weight effect was observed, and it was shown that the high molecular weight modifier was the best emulsifier with a lower critical concentration value for interfacial saturation than the other two. Since higher molecular weight copolymers are considered to be more likely to form micelles, this was taken as an indication that micelle formation for the diblocks, below C_{crit} , was likely not a serious concern in this system. The styrene content of the diblock also influenced its emulsification performance with a 50:50 balanced composition, demonstrating superior emulsification capabilities. A comparison of pure and tapered diblock copolymers did not display any significant differences in emulsification efficacy. In

a recent study¹⁹ which specifically treated the issue of micelle formation, it was shown that essentially all the SEB diblock copolymer goes to the interface in the EPR/PS system, confirming the above observation related to the molecular weight effect. In another related paper,²¹ a technique using electron energy loss spectroscopy (EELS) was developed to identify the location of the modifier in a bromobutyl rubber/polystyrene blend system. This technique, which used an 11–16 nm spot size combined with transmission electron microscope visualization, allows one to locate the interfacial modifier in the blend system.

Having established a basis concerning the emulsification efficacy of a series of modifiers, our most recent papers^{18,19} have examined the fracture performance of these same systems. In one of those papers¹⁸ it was shown that a hydrogenated SEBS triblock copolymer of M_n 50 000 resulted in a significant increase in the impact strength of PS/EPR blends. It was shown that a brittle-ductile transition was closely associated with the saturation of the interface by interfacial modifier. A higher molecular weight triblock (M_n 174 000) was shown to not be as effective an emulsifier as the low molecular weight one. Hence, it had little effect on the mechanical properties of the system.

In this study the work is extended to consider well-defined diblock copolymer interfacial modifiers in a PS/EPR system. The emulsification curve is also used to estimate the areal density of these systems as well as identifying the concentration of modifier required to achieve interfacial saturation. The influence of these parameters on the crack growth resistance and Izod impact of the system as well as a comparison to triblock copolymers is then carried out.

Fracture Characterization

Although the global concept of fracture mechanics such as the strain energy release rate is unable to properly describe the fracture process,²²⁻²⁶ it is presently widely used. On the other hand, in the Charpy and Izod tests, only the total energy absorbed by the sample to break can be measured, and it is well-known that this value does not directly correspond to the fracture performance of the material.²⁷⁻²⁹

Brittle fracture occurs when the strain energy stored in the sample up to the point of fracture is much larger than the energy dissipated in the creation of two fracture surfaces. The energy absorbed by the specimen to fracture is that which is elastically stored in the sample. In this type of fracture, the crack accelerates without any additional supply of energy by external forces. The crack grows in an unstable manner with a speed that is much greater than the impact speed. This leads to the phenomenon of shattering of the part in practice.

When a material exhibits a ductile mode of fracture, crack propagation occurs with much lower speed and in a much more stable manner than a brittle fracture. When crack propagation is stable, fracture can only occur with further supply of energy from external loads. This leads to the conclusion that with the same value of the critical strain energy release rate, G_c , and the fracture energy at crack initiation, G_i , the material exhibiting a ductile mode of fracture performs better in terms of impact resistance than a more brittle material.

Table 1. Properties of Materials

material	commercial name	M_n (g/mol)	M_w (g/mol)	density (g/mL)	T_g (°C)	compos styrene (%)
PS	Styron D685	125 000	275 400	1.05	108	
EPR	Vistalon V-504	69 000	173 000	0.85	-38	
S-EB-1	CAP 4745	187 000				26
S-EB-2	CAP 4741	67 000				30
S-EP-1	KRATON G1702	140 000				27
S-EB-S-1	KRATON G1652	50 000				30

For brittle fracture, the critical strain energy release rate, G_c , was determined as²⁷

$$U = G_c B D \phi \quad (1)$$

where U is the energy absorbed by the sample, B and D are respectively the sample width and thickness, and ϕ is a geometrical function which can be evaluated for any geometry by considering the appropriate calibration factor established for precracked samples.³⁰ From the slope of the plot of U versus $BD\phi$, using samples having different initial crack depths to vary ϕ , the fracture energy, G_c , can be obtained.

For semiductile fracture, a mixed stable-unstable period of crack propagation occurs in the same sample during impact fracture, and in this case, the total energy absorbed by the sample to break, U , has been determined:²⁸

$$U = G_{st} A_1 + G_{inst} B D \phi_1 \quad (2)$$

where G_{st} is the average fracture energy during the first stable crack propagation stage, A_1 is the fracture surface area of the first stable crack propagation zone, G_{inst} is the fracture energy at the onset of unstable crack propagation, and ϕ_1 is the calibration factor corresponding to the crack length at the instability of crack propagation. By plotting U/A_1 against $BD\phi_1/A_1$, G_{st} and G_{inst} can be obtained respectively from the intercept and the slope of the straight line.

For the ductile fracture behavior, another approach taking into account the crack initiation and crack propagation energies in the material has been proposed.^{30,31} Assuming that the fracture energy of the polymer with ductile behavior varies linearly with crack extension and is given by

$$G_r = G_i + T_a A \quad (3)$$

in which G_r is the actual fracture energy, G_i is the fracture energy at crack initiation, T_a represents the rate of change of G_r with crack extension, and A is the fracture surface.

Since the energy absorbed by the specimen is mainly dissipated in the fracture process, the energy absorbed by the specimen becomes

$$U = \int_A G_r dA = G_i A + 0.5 T_a A^2 \quad (4)$$

From this equation one can obtain G_i by the intercept and T_a by the slope of the U/A versus A plot.

Experimental Section

Materials. The system investigated consists of a matrix of polystyrene (PS), supplied by Dow Chemical (Styron D685), and a minor phase of ethylene-propylene rubber (EPR), a random copolymer containing 54% ethylene, supplied by Exxon Chemical (Vistalon V-504). The interfacial agents were supplied by Shell Development Co. They consist of two diblock copolymers of poly(styrene-hydrogenated butadiene), S-EB-1

Table 2. Comparison of the Morphologies Obtained in Different Melt-Processing Environments for the 20% S-EB-2 Copolymer in PS/EPR

	d_n (μm)	d_v (μm)
twin-screw extrusion	0.32	0.42
twin-screw/injection molding ^a	0.43	0.55
Brabender	0.39	0.53

^a Sample taken in core.

and S-EB-2 (CAP 4745 and CAP 4741), and a third diblock consisting of poly(styrene-hydrogenated polyisoprene), S-EP-1 (Kraton G1702). A styrene-hydrogenated butadiene triblock copolymer (S-EB-S-1) was also investigated. The percent styrene in the copolymers is given in Table 1. The number-average molecular weights of S-EB-1 and S-EB-2 are 187 000 and 67 000 g/mol, respectively. The copolymer S-EP-1 has a high number-average molecular weight, $M_n = 140 000$ g/mol. The S-EB-S-1 triblock copolymer has a molecular weight of 50 000 g/mol. All these modifiers are essentially monodisperse. The ethylene-butylene block contains about 35–40% polybutylene; the high polybutylene content inhibits the crystallization of the copolymer. Some properties of these materials are listed in Table 1. The rheological properties of the PS and the EPR have been reported in a previous paper.⁸

Blends. The PS matrix and EPR minor phase were blended in volumetric proportions of 80:20. Blends were prepared with interfacial agent concentrations of 0, 2.5, 5, 10, 15, 20, and 30% based on the minor phase. Thus, the sample containing 10% interfacial modifier has the following composition: 80 parts PS, 20 parts EPR, and 2 parts (10% of EPR content) interfacial modifier. About 0.1 wt % of Irganox 1010 antioxidant (Ciba-Geigy) was also added to the blends.

Morphological Analysis. Emulsification curves were obtained for blends prepared in a Brabender internal mixer. The emulsification study is carried out on the Brabender since it allows for better temperature control and more uniform flow fields and requires small batch sizes. A separate analysis of the 20% S-EB-2 interfacial modifier system (percent based on the dispersed phase) showed that the particle size obtained in the Brabender for the interfacially modified system was very similar to that obtained in the twin screw and in the core of the injection molded pieces destined for impact testing (see Table 2). This justifies the use of the Brabender for the emulsification study and also allows these results to be compared to a whole series of investigations^{8,16–19} carried out on PS/EPR.

All the components of each blend were dry blended before melt mixing. The components were then melt blended for 8 min at 50 rpm and a temperature of 200 °C, before being quenched in cool water. Plane surfaces were obtained for each sample using a Leica model Jung RM 2065 microtome equipped with a glass knife. Samples were held under -100 °C with a stream of liquid nitrogen to minimize surface deformation while cutting. Extraction of the minor phase with a solvent was not required since the rubber particles are ejected from the matrix during cryogenic microtomy.

The samples were then coated with a thin gold-palladium layer prior to scanning electron microscopy (SEM). Micrographs were taken using a JEOL model T300 scanning electron microscope at 10.0 kV. Diameters were determined from surface area measurements, using a semiautomatic analysis method, developed in-house and described elsewhere.³² For each sample, the number-average diameter, d_n , and volume average diameter, d_v , were calculated from 250 to 350 individual particle measurements. A correction proce-

ture was applied to account for polydispersity and for the fact that the knife rarely cuts through the particles at their equator. This procedure was developed by Saltikov.³³ The uncertainty on the average diameter measurements in this case is better than $\pm 4\%$.

SEM observation in the longitudinal direction of the injection molded samples revealed that they display a distinct skin/core progression in the morphology. The EPR particles are highly elongated through the first 0.8–1.2 mm of the samples, at which point a few spherical particles appear. This transition from elongated to spherical particles occurs through the next 0.4 mm, after which nearly all the particles are approximately spherical (core). This skin/core morphology did not seem to depend on the amount of interfacial modifier. To distinguish the influence of the skin, both notched and unnotched Izod impact tests were carried out.

Melt Processing Preparation for Mechanical Property Analysis. The blends for mechanical property analysis were prepared using twin-screw compounding followed by injection molding. The matrix, minor phase, and interfacial agent were blended using a Leistritz AG twin-screw extruder, model 30.34 ($L/D = 28$) operating at 100 rpm. The temperature of the screws and the die was maintained at 200 °C. The extrudate was then quenched in cold water and granulated. The granules were then molded into 6 mm thick plates using a Battenfeld 80 ton injection molding machine, equipped with a Unilog 8000 interface. Injection molding conditions are given in Table 3. Rectangular plates of $127 \times 76 \times 6$ mm were then molded by injection from the extruded material.

Impact Tests. Both Charpy and Izod impact tests were carried out. It is important to note that it is only in the Charpy tests where we study the crack growth resistance. In that case a well-defined notch was prepared, and the strain energy release rate was estimated according to the protocols described below. The Izod tests are included in order to demonstrate the fracture energy by a second technique often used by industry.

Three-point bending impact tests (Charpy tests) were done on a Monsanto plastic impact machine. The calculated hammer speed at the beginning of the impact was 2.5 m/s. Three-point-bend samples of $50 \times 10 \times 6$ mm were cut from the molded plate, parallel to the melt flow direction. To avoid the edge interface on the measured properties, a few millimeters of material was cut off all around the plate. Sharp notches of different lengths were made on three-point-bend samples in two steps: In the first step, a prenotch was made by a saw cut, and in the second step a razor blade was forced into the specimen with a vise. The initial crack length was varied between 20 and 80% of sample width. To reduce the bouncing effect of the sample on the striker during impact, a small amount of plasticine was placed on the striker. The tests were carried out at room temperature and with a humidity of about 50%. After impact the two halves of the test sample were collected to measure the crack length. This measurement was carried out on an optical microscope at a magnification of $12\times$.

Izod impact tests were performed on unnotched and notched samples. The bars were cut from injection-molded 6 mm thick plate to a length and width of 60 mm and 12 mm, respectively. Then they were notched at 3.2 mm for the notched tests. The tests were done on a Custom Scientific Instruments model CS-137C impact tester. The apparatus was equipped with a 542 and 923 g pendulum for notched and unnotched tests, respectively. The units of energy for an Izod impact test are typically reported in J/mm since the ASTM standard defines a constant thickness of sample.

Notched impact testing eliminates the effect of the skin morphology and measures effects directly in the core which possesses spherical-type particles. In the previous study¹⁸ it was shown that a notched Charpy test and unnotched Izod demonstrated all the same essential features related to impact strength improvement as a function of interfacial modifier concentration. To confirm that observation and rigorously determine the effect of the skin, if any, a separate comparison of notched and unnotched Izod impact analysis was also carried out in this study.

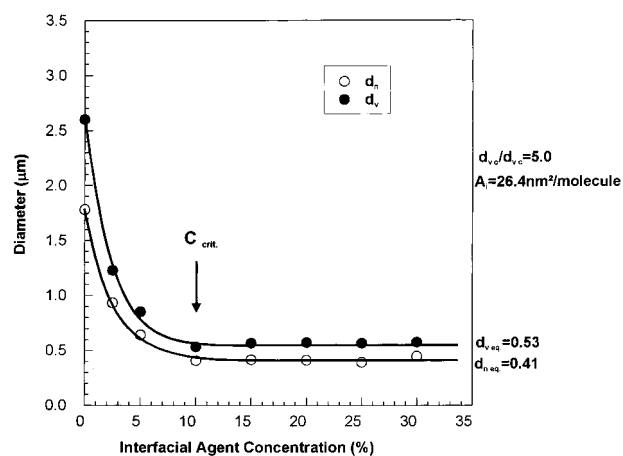


Figure 1. Emulsification curve for blends of 80% polystyrene and 20% ethylene-propylene compatibilized with S-EP-1. The critical concentration for interfacial saturation is shown by an arrow. The percent interfacial modifier concentration is based on the volume of minor phase.

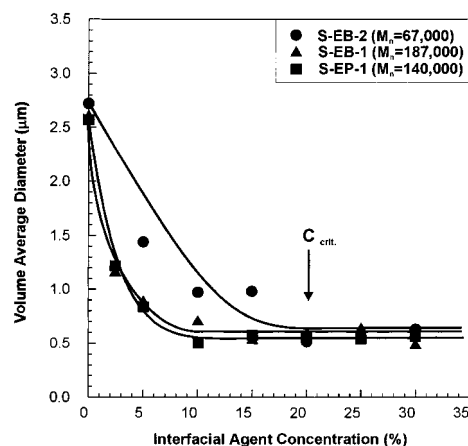


Figure 2. Emulsification curves for blends of 80% polystyrene and 20% ethylene-propylene compatibilized by S-EB-1, S-EB-2, and S-EP-1 diblock copolymers. The critical concentration for interfacial saturation of S-EB-2 is shown by an arrow. The percent interfacial modifier concentration is based on the volume of minor phase.

Results and Discussion

Emulsification of Diblock Copolymers. To separate out the role of emulsification from fracture performance, a series of emulsification curves, carried out on the Brabender mixer, were generated for the PS/EPR and three different diblock interfacial modifiers. The results for S-EP-1 and S-EB-1 are shown in Figures 1 and 2. Both of these modifiers are of similar molecular weight but differ only in the chemical composition of the block (ethylene-propylene vs ethylene-butylene). It is shown unambiguously that both of these modifiers are excellent emulsifiers for the EPR/PS system. In both cases the particle size is reduced by a factor of 5. The curves closely overlap (see Figure 2), with an identical equilibrium particle diameter beyond the C_{crit} and similar values of interfacial area occupied per molecule, A_i (see Table 4). It is clear that substitution of propylene for butylene in the copolymer has no substantial effect on emulsification of the EPR/PS system. Typical SEM photomicrographs are shown in Figure 3.

In Figure 2 the above copolymers are also compared to an emulsification curve for a lower molecular weight copolymer, S-EB-2. It is interesting to note that S-EB-2

Table 3. Injection Molding Conditions

temperature profile (°C)	240/230/210/180
mold temperature (°C)	60
injection pressure (bar)	125
injection speed (mm/s)	50
screw speed (rpm)	40
holding time (s)	20
holding pressure (bar)	70
back-pressure (bar)	1
metering stroke (mm ⁻¹)	75
cooling time (s)	60

also displays the identical steady-state particle size as the other copolymers beyond C_{crit} . Two distinguishing features should be noted, however; first, at lower concentrations of emulsifier S-EB-2, the particle size is significantly higher than the other two higher molecular weight modifiers, and also the C_{crit} is achieved at a higher value. Both of these aspects are consistent with work reported previously on the emulsification of diblock copolymers.¹⁶ From thermodynamic arguments, Noolandi and Hong^{13,14} predicted that the efficacy of a diblock copolymer to compatibilize a blend of immiscible homopolymers would increase with increasing molecular weight. Longer chains would increase the thickness of the interface, which would decrease the enthalpy of the system. Israels et al.³⁴ have also demonstrated that high molecular weight copolymers are more effective at reducing the interfacial tension and thus are better emulsifiers. In a recent paper³⁵ the relative role of interfacial tension reduction and reduced coalescence on particle size reduction in the presence of an interfacial modifier was studied for a similar system as in this paper. In the very high molecular weight range of interfacial modifiers (as used in this work), that study suggests that there is little effect of the molecular weight of the modifier on interfacial tension reduction. If this is the case, then the differences between the copolymers observed in the emulsification curves in Figure 2 are likely related to their ability to reduce coalescence.

A higher C_{crit} value for the 67 000 molecular weight diblock, S-EB-2, in Figure 2 is obtained because at low molecular weight more molecules are required to saturate the same interfacial area. Its interfacial area occupied per molecule at interfacial saturation is shown in Table 4. Since micelle formation is highly sensitive to increasing molecular weight,^{36,37} the fact that the higher molecular weight modifier, S-EB-1 in Figure 2, displays even better emulsification than the low molecular weight one, S-EB-2, indicates that very little micelle formation is occurring here and that the modifiers have a strong affinity for the interface. These results confirm a recent, more detailed study on micelle formation in these systems¹⁹ which indicated that essentially all the diblock copolymer is situated at the interface. This latter point is very important since it means that the areas occupied per molecule for the various interfacial modifiers indicate a true copolymer density at the interface. The areas occupied per molecule (nm² per molecule) at interfacial saturation and their corresponding areal densities (no. of chains per nm²) are shown in Table 4. Figure 4 illustrates the areal density of modifier at the interface as a function of percent interfacial modifier in the blend for the three diblock copolymers. The areal density curve for each copolymer stops once it has achieved interfacial saturation.

A separate analysis of the 20% S-EB-2 interfacial modifier system (percent based on the dispersed phase)

showed that the particle size obtained in the Brabender for the interfacially modified system was very similar to that obtained in the twin-screw and in the core of the injection molded pieces destined for impact testing (see Table 2). Although significant differences in the morphology between Brabender and twin-screw extrusion mixing have been observed in the past for uncompatibilized blends,³⁸ addition of an interfacial modifier or reduction of the viscosity ratio often has the effect of wiping out these differences^{38,39} as in the present case. Care should be taken to verify this particular point for each blend system.

Fracture Performance of Diblock Copolymers.

The fracture performance of these EPR/PS systems was studied via two techniques: crack growth resistance in Charpy impact, including the calculation of G_c and G_i values, and standard Izod impact test analysis as used in industry. Notched impact testing eliminates the effect of the skin morphology and measures effects directly in the core which possesses spherical type particles. In the previous study¹⁸ it was shown that a notched Charpy test and unnotched Izod demonstrated all the same essential features related to impact strength improvement as a function of interfacial modifier concentration. To confirm that observation and rigorously determine the effect of the skin, if any, a separate comparison of notched and unnotched Izod impact analysis was also carried out in this study.

The results for the Charpy and Izod impact are shown in Figures 5–7. It can be seen quite clearly that the low molecular weight diblock modifier (S-EB-2) demonstrates superior performance to either the S-EP-1 or the S-EB-1 high molecular weight copolymers. At 20% of S-EB-2 interfacial modifier, which represents the critical concentration for interfacial saturation from the emulsification curve, a brittle to ductile transition is observed in the Charpy test (Figure 5). This is confirmed in both the notched (Figure 6) and unnotched (Figure 7) Izod impact tests where, at the critical concentration for saturation of the interface, the Izod impact for the system containing S-EB-2 copolymer displays a significant increase as well as a transition from brittle to ductile behavior. This transition to ductile behavior can be attributed to an interfacial effect since the dispersed particle sizes for all three interfacial modifiers are essentially identical at 20% interfacial modifier (see Figure 2). The influence of morphology is thus effectively separated out in these experiments. Since the material is ductile, the G_i calculation was carried out to estimate its fracture energy at crack initiation in Figure 5. To explain the similar G_i and G_c values in Figure 5, as opposed to important increases in impact as measured by Izod testing, one should keep in mind, as mentioned in the Fracture Characterization section, that G_i is the fracture energy at crack initiation. With the same value of the critical strain energy release rate, G_c , and the fracture energy at crack initiation, G_i , the material exhibiting a ductile mode of fracture performs significantly better in terms of impact resistance than a more brittle material. It is interesting to note that at high values of modifier content, above the critical concentration for saturation of the interface, the G_i value in Figure 5 increases substantially. This is also confirmed from the Izod impact tests in Figures 6 and 7.

Figure 5 shows that both S-EB-1 and S-EP-1 display only brittle fracture behavior with a slight increase in G_c at low interfacial modifier content followed by little

Table 4. Areal Densities of the Various Interfacial Modifiers at Interfacial Saturation

type of interfacial agent	composition styrene (%)	M_n (g/mol)	A_i (nm ² /mol)	mol areal density (chains/nm ²)	joint areal density (joints/nm ²)
diblock S-EB-1	26	187 000	30	0.033	0.033
diblock S-EP-1	27	140 000	26	0.038	0.038
diblock S-EB-2 ^a	30	67 000	5.6	0.18	0.18
triblock S-EB-S-1 ^b	30	50 000	13	0.077	0.15

^a Reference 16. ^b Reference 8.

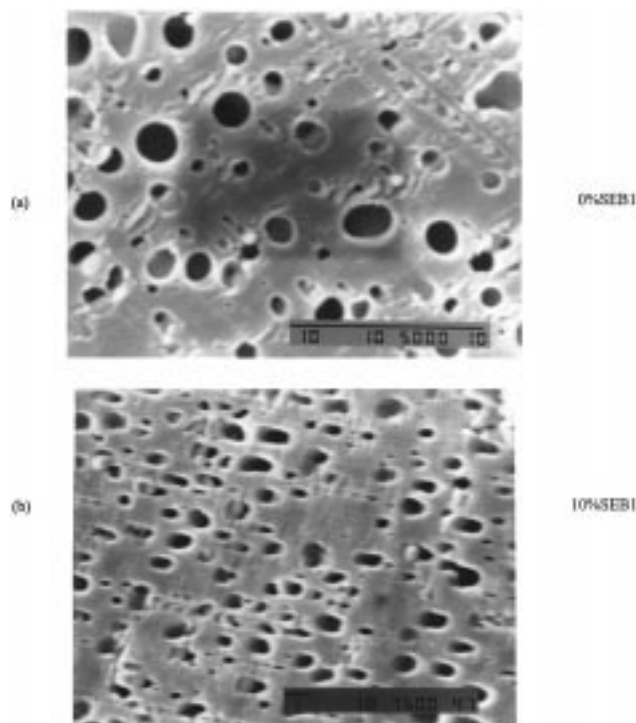


Figure 3. Typical SEM micrographs of dispersed ethylene-propylene in a polystyrene matrix: (a) uncompatibilized; (b) compatibilized with 10% interfacial modifier S-EB-1.

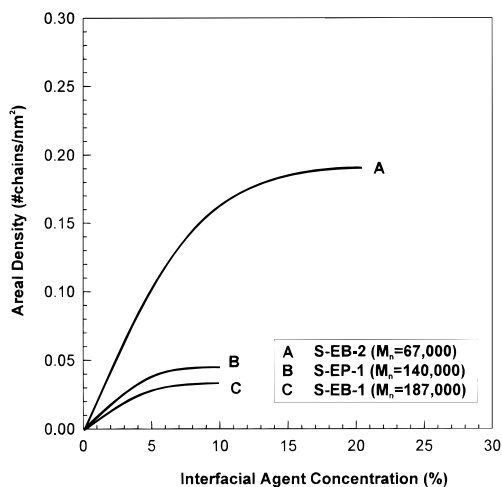


Figure 4. Areal density of the interfacial modifiers as a function of interfacial agent concentration. The percent interfacial modifier concentration is based on the volume of minor phase.

change afterward. This brittle behavior persists even above the critical concentration for interfacial saturation, despite their excellent emulsification capability as shown in Figure 2.

In a previous study,³ Creton, Brown, and Deline studied the influence of a poly(methyl methacrylate) (PMMA)/polystyrene (PS) block copolymer on the frac-

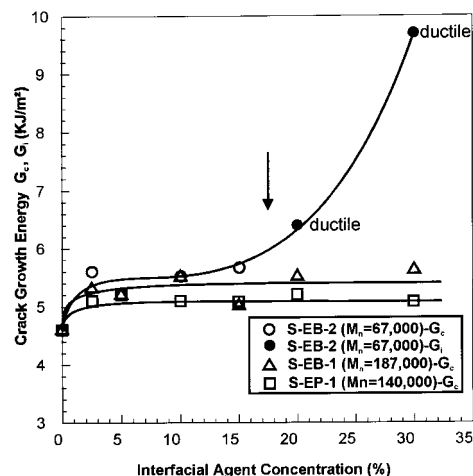


Figure 5. Results of the Charpy crack growth energy for blends of 80% PS and 20% EPR compatibilized by S-EB-1, S-EB-2, and S-EP-1 diblock copolymers. The G_c calculation is used for brittle and G_i for ductile materials. The onset of interfacial saturation for S-EB-2, as determined from Figure 2, is indicated with an arrow.

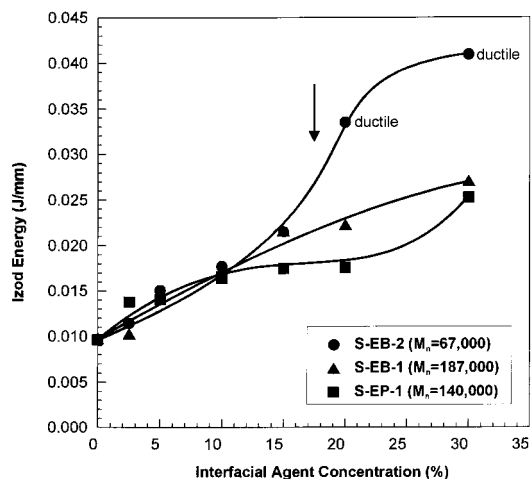


Figure 6. Results of the notched Izod energy for blends of 80% PS and 20% EPR compatibilized by S-EB-1, S-EB-2, and S-EP-1 diblock copolymers. The onset of interfacial saturation for S-EB-2, as determined from Figure 2, is indicated with an arrow.

ture behavior of an immiscible PMMA/poly(phenylene oxide) (PPO) system. A PS/poly(2-vinylpyridine) (PVP) blend modified by a poly(styrene-*b*-2-vinylpyridine) copolymer was also studied by Creton et al.⁴ They describe two principal factors that influence the fracture performance of a blend: the molecular weight of the block and areal density of chains at the interface (Σ). Four main microscopic mechanisms were defined:

(I) For short copolymer chains (below the entanglement molecular weight) the interface failed by a "pull-out" mechanism without any significant amount of plastic deformation.

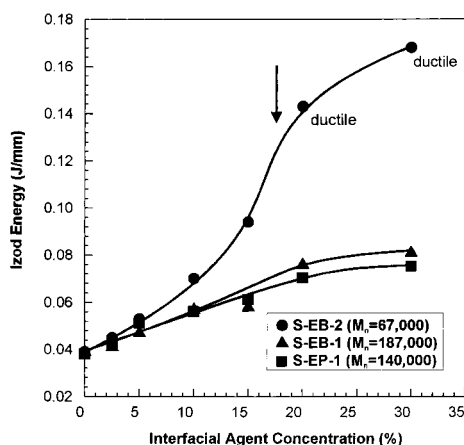


Figure 7. Results of the unnotched Izod energy for blends of 80% PS and 20% EPR compatibilized by S-EB-1, S-EB-2, and S-EP-1 diblock copolymers. The onset of interfacial saturation for S-EB-2, as determined from Figure 2, is indicated with an arrow.

When $P_{PVP} > N_e$ PVP (greater than the entanglement molecular weight) three regimes are possible:

(II) For low Σ , the interface failed without significant amount of plastic deformation. The block copolymer chains break very close to their midpoint, resulting in low values for G_c .

(III) At somewhat higher Σ , the interface fails by the breakdown of the craze fibrils which break by scission of the block copolymer chains close to the joint area.

(IV) For higher Σ , beyond interfacial saturation, the brush region becomes the weakest part of the interface. The fibrils of the craze fail by chain scission in the brush region.

In that study the maximum G_c was obtained at an areal density value of 0.2 very close to the region that they determined for the saturation of the interface. Creton et al.³ report a diminishing G_c value with further increases of modifier since failure then occurs in the brush region (multilayers of modifier form). In their case the modifier was placed directly at the interface and was added to the homopolymer surface using a spin-coating technique. For this reason any modifier in excess of interfacial saturation results in multilayer formation.

In this study, S-EB-1, S-EB-2, and S-EP-1 copolymers all possess blocks with molecular weights that surpass their entanglement density.⁴⁰ Furthermore, the dispersed particle sizes for all three interfacial modifiers are essentially identical at 20% interfacial modifier (see Figure 2). The influence of morphology is thus effectively separated out in these experiments. The poor mechanical performance of the S-EB-1 and S-EP-1 and the improved behavior for S-EB-2 can be understood by comparing the significantly different areal densities of modifier at the interface (Table 4 and Figure 4). At the critical concentration for saturation of the interface, S-EB-1 and S-EP-1 have areal densities of 0.033 and 0.038, respectively, compared to the value for S-EB-2, which is 0.18. Furthermore, the brittle–ductile transition in Figures 5–7 is closely associated with the region of interfacial saturation as determined from the emulsification curve (Figure 2). In a study on the influence of diblock copolymers it was shown that tapered styrene/ethylene–butylene diblocks of M_n 34 000, 64 000, and 136 000 resulted in areal densities of 0.29, 0.16, and 0.041 at interfacial saturation. In a study on triblock copolymers, it was shown that triblocks of 50 000,

70 000, and 174 000 molecular weight resulted in areal densities of 0.077, 0.056, and 0.022 at interfacial saturation. Creton et al.³ report a maximum G_c at an optimum areal density of about 0.2 chains/nm² and interfacial saturation at 0.14 chains/nm² for the PMMA/PPO system modified by the PMMA–PS block copolymer. It appears that areal densities in the range for optimal performance as described by Creton et al. are only achieved with lower molecular weight copolymers under melt-blending conditions. Recent interfacial tension studies from this group³⁵ indicate that addition of the modifier rarely brings the interfacial tension to zero, but rather to a finite plateau value. This indicates strongly that these melt-blended systems are a more open, less modifier dense, intermediate dry–wet brush-type system with significant homopolymer penetration into the interphase region. In the case of Creton et al.,³ the modifier was placed directly at the interface and was added to the PVP surface using a spin-coating technique. This results in important differences as compared to a melt-blended system. Since the modifier is applied from solution, significantly more modifier can be placed at the interface using their technique, as demonstrated by the very high areal density achieved for their high molecular weight modifier.

This work strongly indicates that higher molecular weight copolymers will rarely be able to achieve the areal densities required to optimize performance in melt-blended systems. The best option in a melt-blending operation may be to use lower molecular weight polymers that are of high enough molecular weight to be above their entanglement molecular weight, but low enough to have a significantly high areal density at the interface. The use of lower molecular weight copolymers will also result in the advantage that it will minimize the chances of micellar formation below the critical concentration value and accelerate polymer–polymer interdiffusion.

In Figure 5, the increase of G_i beyond the critical concentration for S-EB-2 is different than what was observed for another PS system studied in the past.¹⁰ In that previous study, a significant increase in impact strength was observed at the critical concentration with no significant change occurring afterward. In this study, however, the interfacial modifier is also an impact modifier in and of itself. In this melt-blended system, once the interface is saturated, excess modifier will form micelles in the system,¹⁹ and it is likely that these micelles exert a synergistic effect on the impact strength of these blends. This important aspect is the subject of continuing study in this group.²⁰ It is interesting to note that Creton et al.³ observe a drop in G_c with values of modifier in excess of interfacial saturation. As mentioned earlier, their spin-coating technique which places the modifier right at the interface results in weak multilayer formation once the interfacial saturation concentration has been surpassed, a phenomenon significantly different from systems prepared under melt-blending conditions.

In comparing the notched and unnotched Izod impact tests, it is interesting to note in Figures 6 and 7 that all the essential features of impact improvement are identical. Both tests demonstrate (1) the improved performance of the S-EB-2 copolymer as compared to S-EB-1 and S-EP-1, (2) the same overall increase in impact for S-EB-2, and (3) the same concentration range for the S-EB-2 brittle to ductile transition. It appears

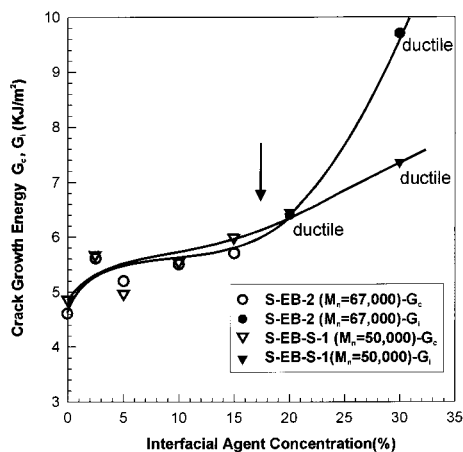


Figure 8. Results of the Charpy crack growth energy for blends of 80% PS and 20% EPR compatibilized by the S-EB-2 diblock copolymer and the S-EB-S-1 triblock copolymer. The G_c calculation is used for brittle and G_i for ductile materials. The onset of interfacial saturation for S-EB-2 and S-EB-S-1 is indicated with an arrow.

to be quite clear that the relatively small skin region does not have a significant effect on the impact strength.

Diblock vs Triblock. In a previous study¹⁸ the influence of triblock copolymers was also studied using an identical approach as this work. In that case, it was clearly shown that the high molecular weight triblock ($M_n = 174\,000$) had a strong propensity for micelle formation and that this hindered its ability to find the interface. In the case of the lower molecular weight triblock, S-EB-S-1 ($M_n = 50\,000$), it was shown via the emulsification curve that, not only was it a good emulsifier, it was also able to improve the mechanical properties of the system once interfacial saturation is achieved. The system was studied using the same protocols as this work, and the fracture behavior was analyzed using a Charpy crack growth resistance study and Izod testing.

In another study⁸ on the emulsification efficacy of triblocks, it was shown that the S-EB-S-1 triblock copolymer occupies 13 nm^2 per molecule at the interface in the absence of micelle formation. This yields an areal density of 0.077 chains per nm^2 (see Table 4). However, the triblock is expected to possess two joints across the interface per modifier molecule, and hence the actual joint density across the interface should be 0.15 joints per nm^2 . Such a value compares closely with the areal density at interfacial saturation of 0.18 for the $67\,000$ molecular weight diblock copolymer in this study. This therefore allows for a comparison of diblock and triblock copolymers where the numbers of joints across the interface are similar and their areal densities are significantly high. Note that the PS block in the diblock ($M_n = 20\,500$) is above the entanglement molecular weight of polystyrene ($M_e = 13\,000$) while the PS block in the triblock ($M_n = 7500$) is well below it.⁴⁰

The results of the Charpy test for both the diblock and triblock copolymers are shown in Figure 8. The results of the Izod impact are shown in Figure 9. It is important to note that both the triblock and the diblock display similar features. First, a small improvement in mechanical properties is observed up to the critical concentration for saturation of the interface. At the C_{crit} (interfacial saturation) both modifiers provoke a brittle-ductile transition in the EPR/PS system. The Izod impact tests in Figure 9 also confirm this with the

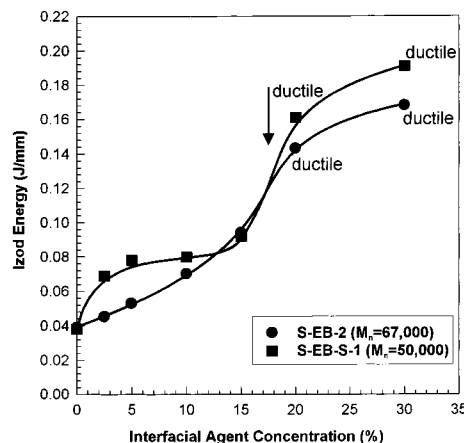


Figure 9. Results of the unnotched Izod energy for blends of 80% PS and 20% EPR compatibilized by the S-EB-2 diblock copolymer and the S-EB-S-1 triblock. The onset of interfacial saturation for S-EB-2 and S-EB-S-1 (same value), as determined from Figure 2 and a previous study,¹⁸ is indicated with an arrow.

impact increasing substantially at the C_{crit} . Furthermore, above the C_{crit} there is an improvement in properties in both cases, once the modifier forms micelles in the system. It is fascinating to observe the virtually identical behavior for both the diblock and triblock copolymer modifiers. These results strongly suggest that the criterion of being above the entanglement molecular weight is not an absolute necessity to achieving a brittle-ductile transition.

Taken all together, these results indicate that it is the number of joints across the interface (areal density of joints) and saturation of the interface that are the most important parameters in optimizing interfaces in melt-processed systems. The present study on diblock copolymers as interfacial modifiers for EPR/PS clearly shows that melt blending is limited in its ability to achieve sufficiently high areal densities at the interface for high molecular weight modifiers. These results may help to explain why graft copolymers have been so successful as interfacial modifiers in melt-blending operations since a given molecular chain has the potential for numerous joints across the interface. It should also be emphasized that this study has focused on aspects related to optimizing interfacial phenomena. In a future work the influence of dispersed phase size will be studied in systems possessing optimized interfaces. The less than expected dependence on the entanglement molecular weight in the melt-blended system as opposed to the model studies carried out previously^{3,4} may be a reflection of the short times involved in melt mixing. A typical mixing cycle in the twin-screw extruder is 1.5 min whereas a typical cycle in injection molding is 1 – 2 min. Taking into account the very slow diffusion times typical for polymer-polymer interdiffusion, it is likely that the short processing times do not allow for the full exploitation of the entanglement molecular weight parameter. Clarifying this important point will be the subject of future work.

Conclusions

In this study both an emulsification and fracture study are coupled to separate out the relative role of emulsification for well-defined diblock copolymer interfacial modifiers in a melt-processed PS/EPR system.

First, very little difference in emulsification efficacy is observed between the SEB and an SEP of similar molecular weight. It is also shown that the addition of a diblock copolymer of molecular weight ($M_n = 67\,000$) to the PS/EPR blend results in a brittle to ductile transition which closely corresponds to the point of interfacial saturation. In contrast, despite their excellent emulsification capabilities, higher molecular weight SEB ($M_n = 187\,000$) and SEP ($M_n = 140\,000$) interfacial modifiers demonstrate only brittle fracture behavior even after interfacial saturation. This poor fracture performance appears to be due to the low areal densities of the higher molecular weight copolymers at the interface. The study underlines that melt blending is limited in its ability to achieve high areal densities for high molecular weight interfacial modifiers. It is shown that the relatively small skin region does not have a significant effect on the impact strength.

A comparison was also made of the effective lower molecular weight diblock from above with a triblock of similar molecular weight. Although the chain areal densities of these two copolymers at the interface are quite different, their areal densities of joints crossing the interface are similar. Both the diblock and triblock copolymers provoke brittle to ductile transitions at interfacial saturation and show virtually identical behavior in both the Charpy crack growth resistance study and Izod impact testing despite the fact that the styrene block in the triblock is below the entanglement molecular weight of polystyrene. These results strongly suggest it is the density of copolymer joints across the interface and interfacial saturation which appear to play the most determining role in the impact strength improvement of interfacially modified melt-blended systems.

Acknowledgment. This work was financed by a Strategic Research Grant obtained by B.D.F. and T.V.K. from the Natural Science and Engineering Research Council of Canada.

References and Notes

- (1) Utracki, L. A. *Polymer Alloys and Blends*; Hanser Publ.: New York, 1989.
- (2) Char, K.; Brown, H. R.; Deline, V. R. *Macromolecules* **1993**, *26*, 4164.
- (3) Creton, C.; Brown, H. R.; Deline, V. R. *Macromolecules* **1994**, *27*, 1774.
- (4) Creton, C.; Kramer, E. J.; Hui, C. Y.; Brown, H. *Macromolecules* **1992**, *25*, 3075.
- (5) Creton, C.; Kramer, E. J.; Hadziioannou, G. *Macromolecules* **1991**, *24*, 1846.
- (6) Gopal, E. S. R. Principles of Emulsion Formation. In *Emulsion Science*; Sherman, P., Ed.; Academic Press: New York, 1968; pp 1–75.
- (7) Djakovic, L.; Dokic, P.; Radivojevic, P.; Sefer, I.; Sovilj, V. *Colloid Polym. Sci.* **1987**, *265*, 993.
- (8) Matos, M.; Favis, B. D.; Lomellini, P. *Polymer* **1995**, *36*, 3899.
- (9) Favis, B. D. *Polymer* **1994**, *35*, 1552.
- (10) Willis, J. M.; Favis, B. D.; Lunt, J. *Polym. Eng. Sci.* **1990**, *30*, 1073.
- (11) Willis, J. M.; Favis, B. D. *Polym. Eng. Sci.* **1988**, *28*, 1416.
- (12) Lepers, J.-C.; Favis, B. D.; Tabar, R. J. *J. Polym. Sci., Polym. Phys.* **1997**, *35*, 2271.
- (13) Noolandi, J.; Hong, K. M. *Macromolecules* **1982**, *15*, 482.
- (14) Noolandi, J.; Hong, K. M. *Macromolecules* **1984**, *17*, 1531.
- (15) Leibler, L. *Makromol. Chem. Macromol. Symp.* **1988**, *16*, 1.
- (16) Cigana, P.; Favis, B. D.; Jérôme, R. *J. Polym. Sci., Polym. Phys.* **1996**, *34*, 1691.
- (17) Favis, B. D.; Cigana, P.; Matos, M.; Tremblay, M. *Can. J. Chem. Eng.* **1997**, *75*, 273.
- (18) Cigana, P.; Favis, B. D.; Albert, C.; Vu-Khanh, T. *Macromolecules* **1997**, *30*, 4163.
- (19) Cigana, P.; Favis, B. D. *Polymer* **1998**, *39*, 3373.
- (20) Odje, S.; VuKhanh, T.; Cigana, P.; Favis, B. D. *Polym. Eng. Sci.*, in press.
- (21) Tremblay, A.; Tremblay, S.; Favis, B. D.; L'Esperance, G.; Selmani, A. *Macromolecules* **1995**, *28*, 4771.
- (22) Sih, G. C.; MacDonald, B. *Eng. Fract. Mech.* **1974**, *6*, 361.
- (23) Sih, G. C. *Eng. Fract. Mech.* **1983**, *5*, 365.
- (24) Sih, G. C.; Madenci, E. *Eng. Fract. Mech.* **1983**, *18*, 1159.
- (25) Gdoutos, E. E.; Sih, G. C. *Theor. Appl. Fract. Mech.* **1984**, *3*, 95.
- (26) Vu-Khanh, T.; Fisa, B. *Theor. Appl. Fract. Mech.* **1990**, *13*, 11.
- (27) Plati, E.; Williams, J. G. *Polym. Eng. Sci.* **1975**, *15*, 470.
- (28) Vu-Khanh, T.; de Charentenay, F. X. *Polym. Eng. Sci.* **1985**, *25*, 841.
- (29) Vu-Khanh, T. *Polymer* **1988**, *29*, 1979.
- (30) Jiang, W.; Liang, H.; Zhang, J.; He, D.; Jiang, B. *J. Appl. Polym. Sci.* **1995**, *58*, 537.
- (31) Vu-Khanh, T. *Theor. Appl. Fract. Mech.* **1994**, *21*, 83.
- (32) Favis, B. D.; Chalifoux, J. P. *Polym. Eng. Sci.* **1987**, *27*, 1591.
- (33) Saltikov, S. A. *Proc. 2nd Int. Congr. Stereol.*; H. Elias: New York, 1967.
- (34) Israels, R.; Jasnow, D.; Balazs, A. C.; Guo, L.; Krausch, G.; Sokolov, J.; Rafailovich, M. *J. Chem. Phys.* **1995**, *102*, 8149.
- (35) Lepers, J.-C.; Favis, B. D. *AIChE J.* **1999**, *45*, 887.
- (36) Vilgis, T. A.; Noolandi, J. *Macromolecules* **1990**, *23*, 2941.
- (37) Whitmore, M. D.; Noolandi, J. *Macromolecules* **1985**, *18*, 657.
- (38) Favis, B. D.; Therrien, D. *Polymer* **1991**, *32*, 1474.
- (39) Gonzalez-Nunez, R.; De Kee, D.; Favis, B. D. *Polymer* **1996**, *37*, 4689.
- (40) Fetters, L. J.; Lohse, D. J.; Richter, D.; Witten, T. A.; Zirkel, A. *Macromolecules* **1994**, *27*, 4639.

MA981481Y